UKRAINIAN JOURNAL OF MECHANICAL ENGINEERING AND MATERIALS SCIENCE

Vol. 5, No. 2, 2019

Vitaliy Korendiy [1], Roman Zinko [2], Yurii Cherevko [3]

1. Department of Mechanics and Automation Engineering, Lviv Polytechnic National University, Ukraine, Lviv, S. Bandery Street 12, E-mail: vitaliy.nulp@gmail.com, ORCID 0000-0002-6025-3013
2. Department of Automotive Engineering, Lviv Polytechnic National University, Ukraine, Lviv, S. Bandery Street 12, E-mail: rzinko@gmail.com, ORCID 0000-0002-3275-8188
3. Research Department of Armored Weapons and Technology, Army Science Center, Hetman Petro Sahaidachnyi National Army Academy, Ukraine, Lviv, Heroes of Maidan Street 32, E-mail: cherevko_um@ukr.net, ORCID 0000-0001-7468-8213

STRUCTURAL AND KINEMATIC ANALYSIS OF PANTOGRAPH-TYPE MANIPULATOR WITH THREE DEGREES OF FREEDOM

Received: April 07, 2019 / Revised: June 27, 2019 / Accepted: August 30, 2019

Abstract. *Problem statement*. The processes of development and improvement of autonomous mobile robots are significantly constrained because of the lack of an open-access comprehensive scientific and theoretical framework for calculating and designing of autonomous mobile robotic systems *Purpose*. The main objective of the paper consists in carrying out kinematic analysis and motion simulation of pantograph-type manipulator with three degrees of freedom. *Methodology*. The method of closed vector loops is used for deriving the equations of motion of the robot's manipulator. In order to perform simulation (virtual experiment), the 3D-model of the robot was designed in SolidWorks software. *Findings (results)*. The motion equations of the pantograph-type manipulator are derived, and the graphical dependencies describing the trajectories (paths) of the gripping device are constructed. In order to substantiate the correctness of the derived equations, and of the presented laws of the gripper motion, the corresponding 3D-model of the robot was designed and investigated in SolidWorks software. *Scopes of further investigations*. In the present paper, there are analysed kinematic parameters of the manipulator motion. While carrying out further investigations, it is necessary to perform its dynamic analysis taking into account all the forces acting upon the elements of the robot, as well as the influence of drives. This will allow to catty out the optimization synthesis of the robots structure, namely the geometrical parameters of the mechanism, operational parameters of drives, etc.

Keywords: structural analysis, kinematic analysis, manipulator, degree of freedom, mobile robot, simulation, robotic system, operational parameters.

Introduction

Robotization of industrial and technological processes in all fields of the human activity is a leading and long-term trend of development of modern society [1]. Nowadays, industrial robots have become quite widespread and have formed the main technological base of the machine-building, instrument-making, electrical and electronic fields of the world's industry [1], [2]. Development of perfect industrial robots is carried out on the basis of scientific research, theoretical and applied investigations performed by scientists of numerous research schools in Ukraine and abroad.

Over the last decades, a new direction of robotics related with autonomous mobile robots equipped by onboard control systems has been formed [3]–[14]. However, the processes of development and improvement of these significantly complicated robotic devices are constrained because of the lack of an open-access comprehensive scientific and theoretical framework for calculating and designing of autonomous mobile robotic systems, taking into account the latest developments in the areas of navigation systems, systems of technical vision, systems of environmental analysis and decision-making, etc. [3]–[14].

Problem Statement

The necessity of widespread implementation of mobile robots is caused by following factors: the improvement of productivity of manufacturing and technological processes and reducing danger to human life; the increase in the number and scale of man-made disasters, which are inevitable in the conditions of industrialization of the economy; an increase in the number of natural and environmental disasters caused by global warming and industrialization; changing the character of modern military operations, in which the role of robotic devices is rapidly growing; increasing the scale and variety of terrorism; increase in production and transportation of drugs, radioactive and other dangerous substances [1]–[5].

There are a number of extreme conditions where the only means capable of protecting human beings are mobile robots. Therefore, for many industries and government institutions, the use of mobile robots is the only way to eliminate or reduce the risk to human life and health [1]–[5]. Ukraine's urgent need for mobile robots is caused by the necessity to equip the army by new models of intelligent precision weapons, to solve a number of problems of the Chernobyl nuclear power plant, including the exclusion zone, and other nuclear power plants, as well as the necessity of disposal of mines, other explosive devices, the disposal of large quantities of ammunition, missiles, rockets fuels. radioactive and poisonous substances etc.

Review of Modern Information Sources on the Subject of the Paper

A modern mobile robot able to perform a number of functions mentioned above is a complex system, in which the latest achievements of many branches of science and technology are combined. The designing and production of mobile robots involves the use of advanced technologies in such scientific and technical areas as compact and energy-intensive sources and energy converters; highly reliable off-road vehicles; high-precision satellite and inertial navigation systems; multi-link technological manipulators with precision programmable drives of high specific power; noise-tolerant multi-channel command and telemetry systems of radio and fiber communication, systems of technical vision; multilevel adaptation systems for remote control of robots and special software of their systems [1]–[14].

One of the other basic directions of development of mobile robots is the improvement of their "mechanical" part in order to increase passability, improve controllability, expand the performed technological operations etc. The latter task largely depends on the design of the manipulator and gripper.

The structure of a manipulator is determined by the location of its drives. If the drives are placed directly in kinematic pairs, then the masses of the drives are added to the masses of the moving parts of the manipulator [5]–[8]. If the total load on the drives and their power increase, then the ratio of the manipulator mass to the payload (maximum mass of the object being manipulated) decreases. Therefore, in the designs of some robots, the hand and arm drives tend to be placed closer to the base of the robot in order to reduce the mass of the robot's movable part and the inertial forces acting upon the links and joints of the manipulator [5]–[8]. In this case, the additional kinematic chains are used to transfer motion from the drive to the corresponding link.

The manipulators using the principle of placing drives on the robot's base have more complex mechanisms. However, an increase in the number of links and kinematic pairs is compensated by a decrease in masses and moments of inertia of the moving links of the manipulator [9], [10]. In addition, closed kinematic chains increase the accuracy and rigidity of the mechanism. In general, manipulators that use the principles of combined arrangement of drives (one part of drives are placed on the base, while the other drives are placed on the movable links) have better energy and dynamic characteristics, as well as higher accuracy [11], [12].

Objectives and Problems of Research

The main objective of this paper consists in structural and kinematic analysis of the pantograph-type manipulator with three degrees of freedom. To achieve this goal, the following tasks will be solved: 1) review of the design and operational features of a mobile robot with a pantograph-type mechanism of a manipulator; 2) analysis of the structure, kinematics and operational parameters of the manipulator; 3) simulation modelling of the gripper motion in MatLab, SolidWorks Motion and MapleSim software.

Design Peculiarities of Mobile Robot

The manufactured mobile robot and its design view developed in SolidWorks software are presented in Fig. 1. The robot consists of the gripping device (clamp, grab, tong etc.) 1, manipulator 2, wheel-type chassis (landing gear) 3, remote control system 4, and feed (power supply) system 5. The gripping device 1 is designed on the basis of the single-degree-of-freedom gear-type mechanism driven by electric motor. Each wheel of the chassis (landing gear) 3 is equipped by the separate electric drive controlled with a help of the ARDUINO hardware 4. The wheels are rigidly fixed on the shafts of the corresponding electric motors. In order to change the motion direction of the robot, there is implemented the possibility of "board rotation", which provides different speeds and directions of rotation of the wheels of the left and right sides of the wheel chassis. The design of the manipulator uses a doubled pantograph-type mechanism with two degrees of freedom to ensure lowering/raising and pushing/pulling of the gripper. The third degree of freedom provides rotation of the manipulator around a vertical axis. The design of the gripper is equipped by a separate drive with a gear transmission to transmit torque from the motor shaft to the gripping levers.

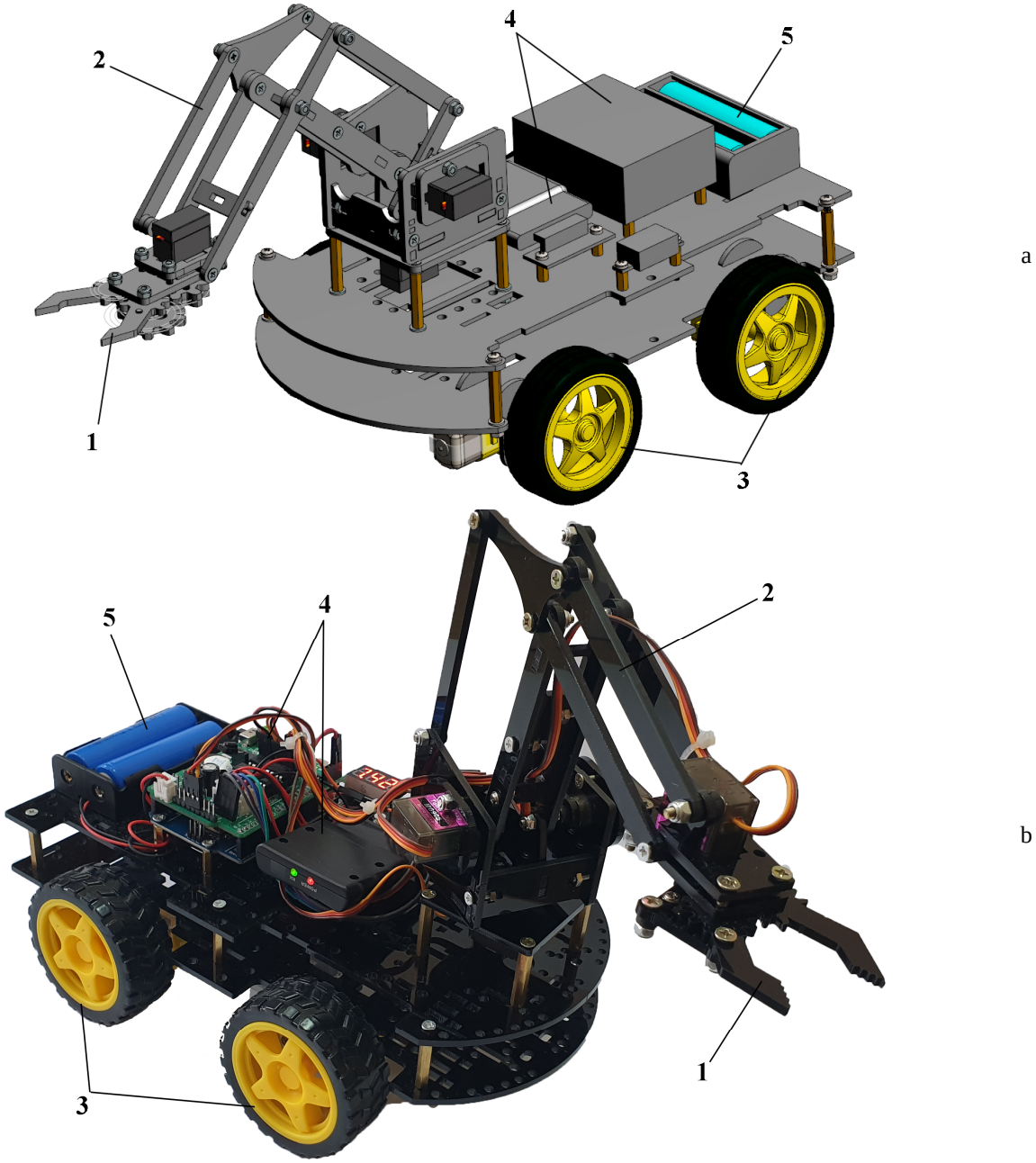

Fig. 1. Manufactured mobile robot (b) and its 3D model designed in SolidWorks software (a)

Structural and Kinematic Analysis of Manipulator

In the manipulator mechanism presented in Fig. 2, a stable horizontal position of the plane S of the gripper is provided with the simultaneous possibility of movement of the manipulator along three coordinates of Cartesian system. The manipulator is placed on the shaft of the electric motor (thrust bearing O), which is rigidly connected to the frame of the mobile (wheeled) transporting platform. To the base of the manipulator, which is able to rotate around the joint O in the horizontal plane, two driving rockers A_2A_{10}, A_4A_5 and one passive rocker A_1A_6 are joined. The connecting rods A_4A_7, A_7A_{13}, $A_{11}A_{14}$, $A_{13}A_{14}$ and A_6A_{11} perform the planar motion (in a vertical plane).

The number of movable links of the considered manipulator mechanism is equal to $n=9$, and the number of single-motion (revolute) kinematic pairs is $p_5=12$. There are no higher kinematic pairs in this manipulator mechanism, i.e. $p_4=0$. The degree of freedom of the mechanism can be determined by the following formula [7], [8]:

$$W=3\cdot n-2\cdot p_5-p_4=3\cdot 9-2\cdot 12-0=3. \tag{1}$$

Therefore, we can state that the considered manipulator mechanism (Fig. 2) has three degrees of freedom. That's why there are three driving links and three independent coordinates, which uniquely determine the position of all the rest links of the mechanism. Let's accept the following driving links: the link OA_3, which rotates around the thrust bearing O; the link A_2A_{10}, which rotates around the joint A_2; the link A_4A_5, which rotates around the joint A_5 (Fig. 2). Then the angles φ_1, φ_2, φ_3 can be considered as the generalized coordinates.

The kinematical analysis of the manipulator mechanism will be carried out using the analytical method of closed vector loops [6]–[9], and MatLab software [13], [14].

Let's accept the following initial position of the mechanism: 1) the axis that passes through the joints A_2, A_3, A_5, is parallel to the axis Oy; 2) the rod A_4A_5 is parallel to the axis Ox; 3) the rod A_2A_{10} is in vertical position. Let's denote the lengths of the links l_{ij}, where i, j are the letters that represent the corresponding link (Fig. 2).

The coordinates of the joints A_2 and A_5 of the driving rod can be determined with a help of the following formulas:

$$\begin{aligned}
&X_{A_2}(\varphi_1)=\left(B_1B_2+B_5A_2\right)\cdot\cos(\varphi_1)+B_2B_5\cdot\sin(\varphi_1);\\
&X_{A_5}(\varphi_1)=\left(B_1B_2+B_4A_5\right)\cdot\cos(\varphi_1)-B_2B_4\cdot\sin(\varphi_1);\\
&Y_{A_2}(\varphi_1)=\left(B_1B_2+B_5A_2\right)\cdot\sin(\varphi_1)-B_2B_5\cdot\cos(\varphi_1);\\
&Y_{A_5}(\varphi_1)=\left(B_1B_2+B_4A_5\right)\cdot\sin(\varphi_1)+B_2B_4\cdot\cos(\varphi_1);\\
&Z_{A_2}=Z_{A_5}=OB_1.
\end{aligned} \tag{2}$$

The coordinates of the joints A_{10}, A_8 та A_4 are as follows:

$$\begin{aligned}
&X_{A_{10}}(\varphi_1,\varphi_2)=\left(B_1B_2+B_5A_2+A_2A_{10}\cdot\sin(\varphi_2)\right)\cdot\cos(\varphi_1)+B_2B_5\cdot\sin(\varphi_1);\\
&X_{A_8}(\varphi_1,\varphi_2)=\left(B_1B_2+B_3A_3+A_2A_{10}\cdot\sin(\varphi_2)\right)\cdot\cos(\varphi_1)-B_2B_3\cdot\sin(\varphi_1);\\
&X_{A_4}(\varphi_1,\varphi_3)=\left(B_1B_2+B_4A_5-B_4A_4\cdot\cos(\varphi_3)\right)\cdot\cos(\varphi_1)-B_2B_4\cdot\sin(\varphi_1);\\
&Y_{A_{10}}(\varphi_1,\varphi_2)=\left(B_1B_2+B_5A_2+A_2A_{10}\cdot\sin(\varphi_2)\right)\cdot\sin(\varphi_1)-B_2B_5\cdot\cos(\varphi_1);\\
&Y_{A_8}(\varphi_1,\varphi_2)=\left(B_1B_2+B_3A_3+A_2A_{10}\cdot\sin(\varphi_2)\right)\cdot\sin(\varphi_1)+B_2B_3\cdot\cos(\varphi_1);
\end{aligned} \tag{3}$$

$$Y_{A_4}(\varphi_1,\varphi_3) = \left(B_1B_2 + B_4A_5 - B_4A_4 \cdot \cos(\varphi_3)\right) \cdot \sin(\varphi_1) + B_2B_4 \cdot \cos(\varphi_1);$$
$$Z_{A_{10}}(\varphi_2) = Z_{A_8}(\varphi_2) = OB_1 + A_2A_{10} \cdot \cos(\varphi_2);$$
$$Z_{A_4}(\varphi_3) = OB_1 + B_4A_4 \cdot \sin(\varphi_3).$$

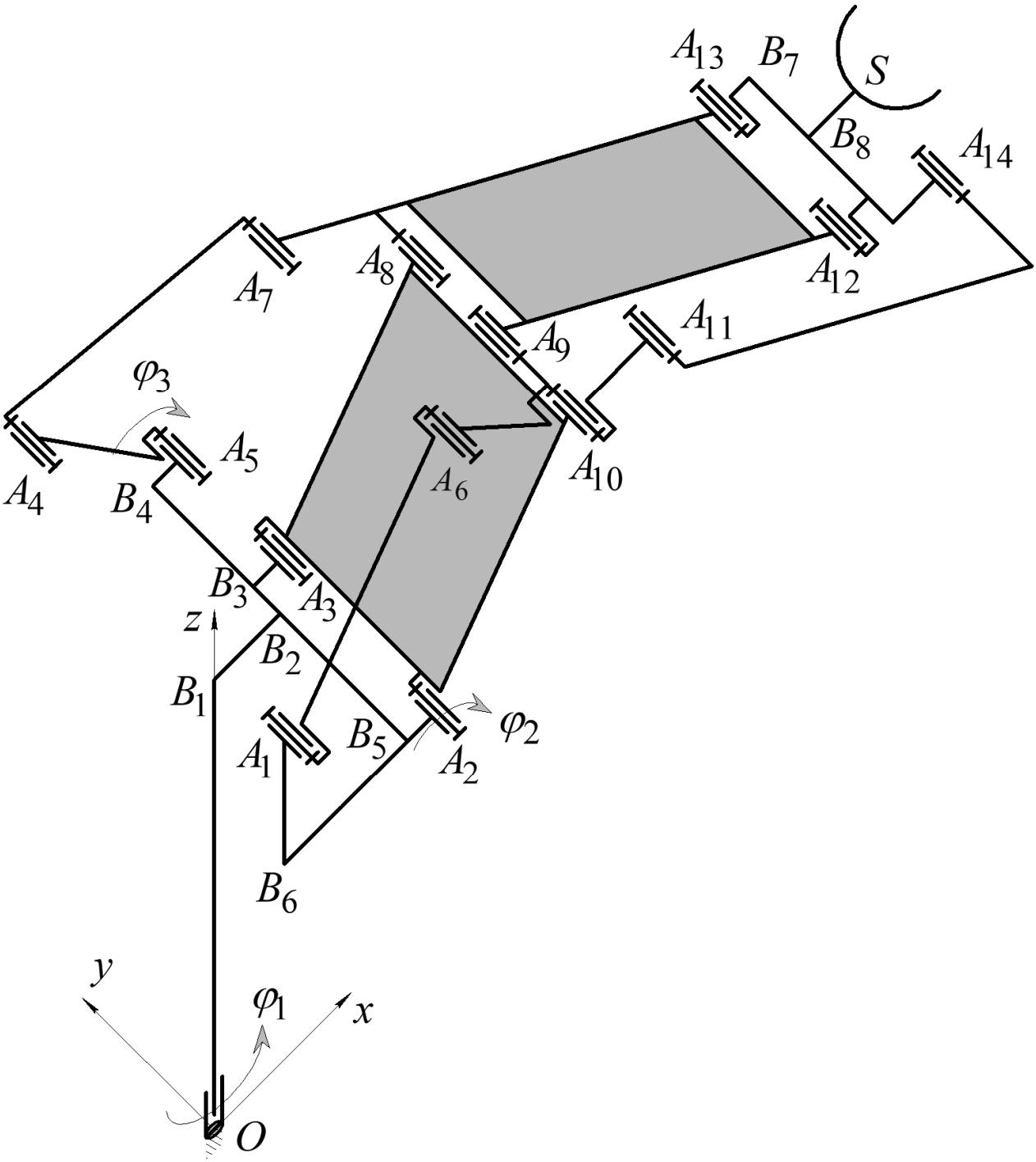

Fig. 2. Structure diagram of the manipulator

In further calculations, let us adopt that the joints A_4, A_5, A_7, A_{13} are located and move in one vertical plane passing through the axis Ox. This allows to simplify the coordinate equations of the corresponding joints by defining the coordinates along the axes Ox and Oz. The coordinates of these joints with respect to the axis Oy will be further easily expressed in terms of coordinates relative to the

axis Ox at a known angle φ_1. To determine the coordinates of the joint A_7 based on the method of closed vector loops, the following equations are derived:

$$X_{A_8}(\varphi_2) = X_{A_9}(\varphi_2) = X_{A_{10}}(\varphi_2) = B_1B_2 + B_5A_2 + A_2A_{10} \cdot \sin(\varphi_2);$$

$$X_{A_4}(\varphi_3) = B_1B_2 + B_4A_5 - B_4A_4 \cdot \cos(\varphi_3);$$

$$Z_{A_8}(\varphi_2) = Z_{A_9}(\varphi_2) = Z_{A_{10}}(\varphi_2) = OB_1 + A_2A_{10} \cdot \cos(\varphi_2);$$

$$Z_{A_4}(\varphi_3) = OB_1 + B_4A_4 \cdot \sin(\varphi_3);$$

$$x_{A_7}(\varphi_2,\varphi_3) = x_{A_8}(\varphi_2) - \frac{\left[\begin{array}{l}\left(x_{A_8}(\varphi_2) - x_{A_4}(\varphi_3)\right)\times \\ \times\left(\left(A_7A_8\right)^2 - \left(A_7A_4\right)^2 + \left(z_{A_8}(\varphi_2) - z_{A_4}(\varphi_3)\right)^2 + \left(x_{A_8}(\varphi_2) - x_{A_4}(\varphi_3)\right)^2\right) + \\ + \left(z_{A_8}(\varphi_2) - z_{A_4}(\varphi_3)\right)\times \\ \times\sqrt{\left[\left(A_7A_8 + A_7A_4\right)^2 - \left(x_{A_8}(\varphi_2) - x_{A_4}(\varphi_3)\right)^2 - \left(z_{A_8}(\varphi_2) - z_{A_4}(\varphi_3)\right)^2\right]\times} \\ \sqrt{\times\left[\left(x_{A_8}(\varphi_2) - x_{A_4}(\varphi_3)\right)^2 + \left(z_{A_8}(\varphi_2) - z_{A_4}(\varphi_3)\right)^2 - \left(A_7A_8 - A_7A_4\right)^2\right]}\end{array}\right]}{2\cdot\left[\left(x_{A_8}(\varphi_2) - x_{A_4}(\varphi_3)\right)^2 + \left(z_{A_8}(\varphi_2) - z_{A_4}(\varphi_3)\right)^2\right]};$$

$$z_{A_7}(\varphi_2,\varphi_3) = z_{A_4}(\varphi_3) - \frac{\left[\begin{array}{l}\left(z_{A_8}(\varphi_2) - z_{A_4}(\varphi_3)\right)\times \\ \times\left(\left(A_7A_8\right)^2 - \left(A_7A_4\right)^2 - \left(z_{A_8}(\varphi_2) - z_{A_4}(\varphi_3)\right)^2 - \left(x_{A_8}(\varphi_2) - x_{A_4}(\varphi_3)\right)^2\right) - \\ - \left(x_{A_8}(\varphi_2) - x_{A_4}(\varphi_3)\right)\times \\ \times\sqrt{\left[\left(A_7A_8 + A_7A_4\right)^2 - \left(x_{A_8}(\varphi_2) - x_{A_4}(\varphi_3)\right)^2 - \left(z_{A_8}(\varphi_2) - z_{A_4}(\varphi_3)\right)^2\right]\times} \\ \sqrt{\times\left[\left(x_{A_8}(\varphi_2) - x_{A_4}(\varphi_3)\right)^2 + \left(z_{A_8}(\varphi_2) - z_{A_4}(\varphi_3)\right)^2 - \left(A_7A_8 - A_7A_4\right)^2\right]}\end{array}\right]}{2\cdot\left[\left(x_{A_8}(\varphi_2) - x_{A_4}(\varphi_3)\right)^2 + \left(z_{A_8}(\varphi_2) - z_{A_4}(\varphi_3)\right)^2\right]}.$$

Having determined the coordinates of the joints A_7 and A_8, we can determine the coordinates of the joint A_{13} (the gripper fixation point) using the following relations:

$$\begin{gathered}\frac{x_{A_{13}}(\varphi_2,\varphi_3) - x_{A_7}(\varphi_2,\varphi_3)}{A_7A_{13}} = \frac{x_{A_8}(\varphi_2) - x_{A_7}(\varphi_2,\varphi_3)}{A_7A_8} \Rightarrow \\ \Rightarrow x_{A_{13}}(\varphi_2,\varphi_3) = \frac{A_7A_{13}\cdot\left(x_{A_8}(\varphi_2) - x_{A_7}(\varphi_2,\varphi_3)\right)}{A_7A_8} + x_{A_7}(\varphi_2,\varphi_3); \\ \frac{z_{A_{13}}(\varphi_2,\varphi_3) - z_{A_7}(\varphi_2,\varphi_3)}{A_7A_{13}} = \frac{z_{A_8}(\varphi_2) - z_{A_7}(\varphi_2,\varphi_3)}{A_7A_8} \Rightarrow \\ \Rightarrow z_{A_{13}}(\varphi_2,\varphi_3) = \frac{A_7A_{13}\cdot\left(z_{A_8}(\varphi_2) - z_{A_7}(\varphi_2,\varphi_3)\right)}{A_7A_8} + z_{A_7}(\varphi_2,\varphi_3).\end{gathered} \tag{4}$$

The coordinates of the gripper supporting point B_8 are as follows:

$$x_{A_{13}}(\varphi_2,\varphi_3) = \left[\frac{A_7A_{13}\cdot\left(x_{A_8}(\varphi_2) - x_{A_7}(\varphi_2,\varphi_3)\right)}{A_7A_8} + x_{A_7}(\varphi_2,\varphi_3)\right]\cdot\cos\varphi_1 + \left(B_2B_4 - B_7B_8\right)\cdot\sin\varphi_1; \tag{5}$$

$$y_{A_{13}}(\varphi_2,\varphi_3)=\left[\frac{A_7A_{13}\cdot\left(x_{A_8}(\varphi_2)-x_{A_7}(\varphi_2,\varphi_3)\right)}{A_7A_8}+x_{A_7}(\varphi_2,\varphi_3)\right]\cdot\sin\varphi_1+\left(B_2B_4-B_7B_8\right)\cdot\cos\varphi_1;$$

$$z_{A_{13}}(\varphi_2,\varphi_3)=\frac{A_7A_{13}\cdot\left(z_{A_8}(\varphi_2)-z_{A_7}(\varphi_2,\varphi_3)\right)}{A_7A_8}+z_{A_7}(\varphi_2,\varphi_3).$$

To determine other kinematic parameters of the manipulator, in particular, the speed and acceleration of the gripper (or the analogues of speed and acceleration), it is necessary to differentiate the dependences (5) with respect to the corresponding generalized coordinates, considering the coordinates as the functions depending on time.

Analyzing the proposed structure diagram of the manipulator (Fig. 2), we can state that the generalized coordinate φ_1 describes the rotation of the manipulator around the vertical axis. The generalized coordinates φ_2, φ_3 describe the raising/lowering and pushing/pulling movements of the gripper.

Numerical Modelling of the Gripper Motion Using the Derived Analytical Dependencies

In order to perform the numerical modelling of the gripper motion let us use the derived analytical dependencies (1) – (5) and accept the following geometrical parameters of the manipulator in accordance with the proposed design (Figs. 1 and 4): $OB_1=35$ mm, $B_1B_2=B_5B_6=10$ mm, $B_2B_4=B_2B_5=B_6A_1=15$ mm, $B_5A_2=B_3A_3=B_4A_5=B_2B_3=5$ mm, $A_1A_6=A_2A_{10}=A_3A_8=A_4A_7=A_9A_{12}=A_{11}A_{14}=80$ mm, $B_4A_4=35$ mm, $A_{10}A_{11}=A_{12}A_{14}=15$ mm, $A_7A_8=35$ mm, $A_7A_{13}=115$ mm, $A_{12}A_{13}=20$ mm, $A_9A_{10}=10$ mm.

Let us model the motion of the supporting point A_{13} in several characteristic positions of the driving rockers A_2A_{10}, A_4A_5: Fig. 3, a – the rocker A_2A_{10} rotates from its vertical position to the horizontal one, while the rocker A_4A_5 is in the initial horizontal position; Fig. 3, b – the rocker A_2A_{10} is in the initial vertical position, while the rocker A_4A_5 rotates from its horizontal position to the vertical one; Fig. 3, c – the rocker A_2A_{10} rotates from vertical to horizontal position, while the rocker A_4A_5 is in vertical position; Fig. 3, d – the rocker A_2A_{10} is in its horizontal position, while the rocker A_4A_5 rotates from its horizontal position to the vertical one.

The considered graphical dependences confirm that the generalized coordinates φ_2, φ_3 describe the raising/lowering and pushing/pulling movements of the gripper. Analysing these dependences, we can conclude that to lower the gripper it is necessary to increase the angles φ_2, φ_3, while to push the gripper (to extend it in the horizontal direction) it is necessary to increase the angle φ_2 or to decrease the angle φ_3.

The proposed mechanism of the manipulator provides a constant horizontality of the working plane of the gripper, that is why in the process of modelling it was enough to choose the supporting hinge of the gripper as a point to be studied, and to use the equations (4).

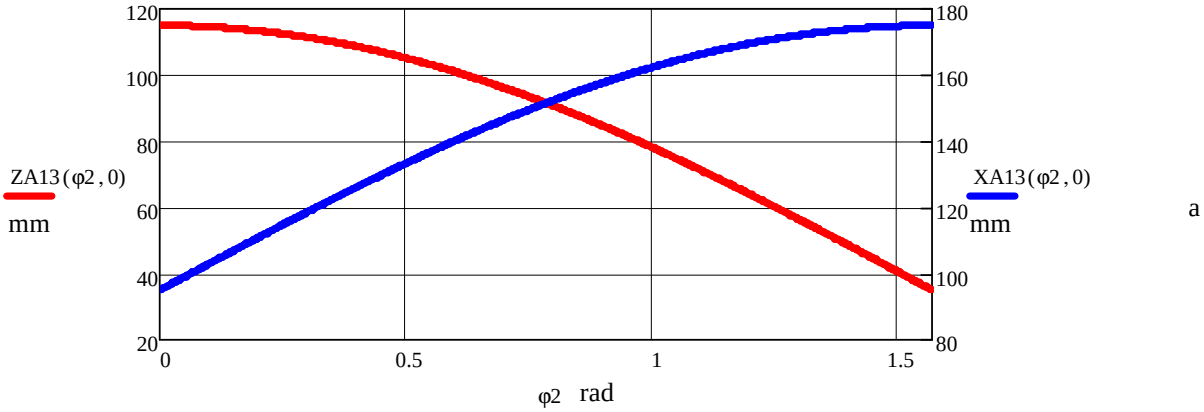

Fig. 3. Graphic dependencies of changing the coordinates of the gripper supporting point while performing the characteristic movements, which were selectively investigated in the process of numerical modelling: a – $\varphi_3 = 0$

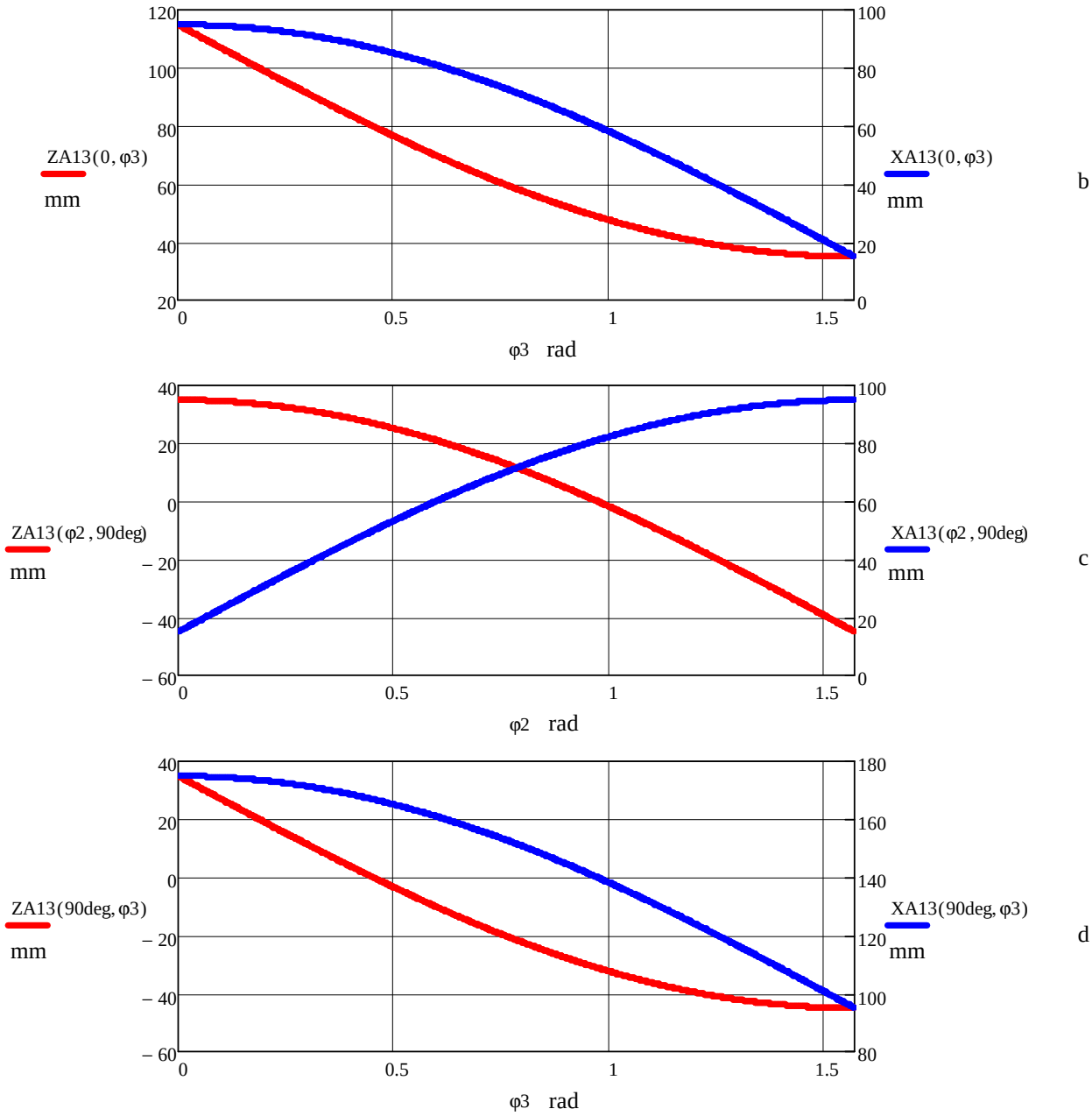

Fig. 3. (Continuation). Graphic dependencies of changing the coordinates of the gripper supporting point while performing the characteristic movements, which were selectively investigated in the process of numerical modelling: b – $\varphi_2 = 0$; c – $\varphi_3 = 90°$; d – $\varphi_2 = 90°$

Simulation of the Gripper Motion in SolidWorks Software

SolidWorks Motion is a software for performing engineering analysis of various mechanical systems. In particular, in our case, this program will allow integrated kinematic analysis and motion simulation of the manipulator (Fig. 4) on the basis of its solid-state model.

In order to confirm the derived analytical dependences (1) – (5) describing the kinematics of the manipulator, as well as to verify the results of numerical simulation of the gripper motion (Fig. 3), in this section we shall perform motion simulation of the manipulator in SolidWorks Motion software and present the results in the form of characteristic positions indicating the appropriate geometric parameters (Fig. 5).

In Fig. 5, a, there is shown the initial position of the manipulator, for which $\varphi_2 = 0$, $\varphi_3 = 0$, i.e. the driving rocker A_2A_{10} is in the vertical position, and the rocker A_4A_5 is in the horizontal position. The obtained geometric parameters completely match the results of numerical modelling presented in Figs. 3, a, b.

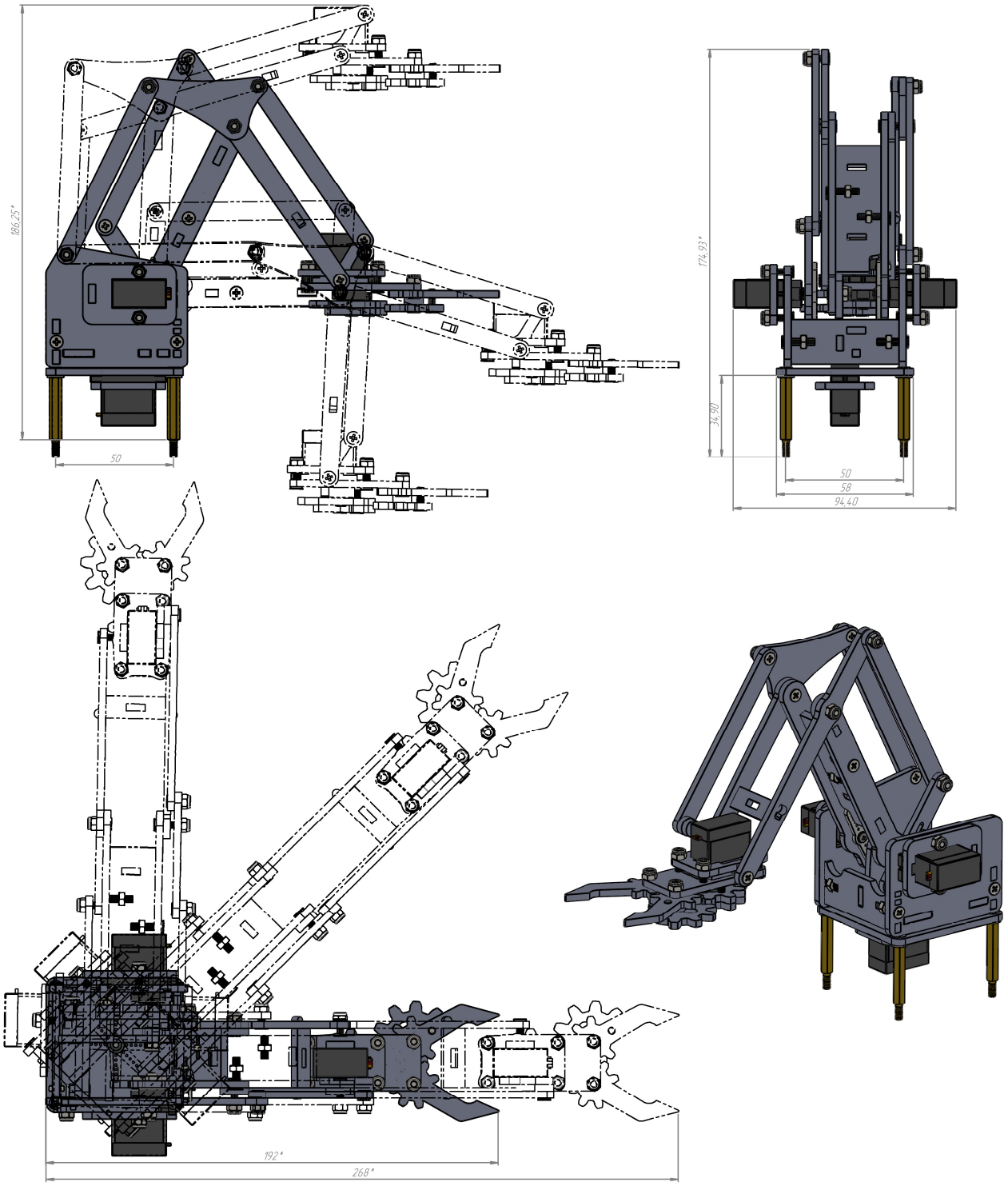

Fig. 4. Design of the manipulator

In Fig. 5, b, there is shown the position of the manipulator, for which $\varphi_2 = 0$, $\varphi_3 = 90°$, i.e. both driving rockers A_2A_{10} and A_4A_5 are in their vertical positions. The obtained geometric parameters completely match the results of numerical modelling presented in Figs. 3, b, c.

Fig. 5, c shows the position of the manipulator, for which $\varphi_2 = 90°$, $\varphi_3 = 0$, i.e. both driving rockers A_2A_{10} and A_4A_5 are in their horizontal positions. The obtained geometric parameters completely match the results of numerical modelling presented in Fig. 3, a, d.

In Fig. 5, d, there is shown the position of the manipulator, for which $\varphi_2 = 90°$, $\varphi_3 = 90°$, i.e. the driving rocker A_2A_{10} is in the horizontal position, and the rocker A_4A_5 is in the vertical position. The obtained geometric parameters completely match the results of numerical modelling presented in Fig. 3, c, d.

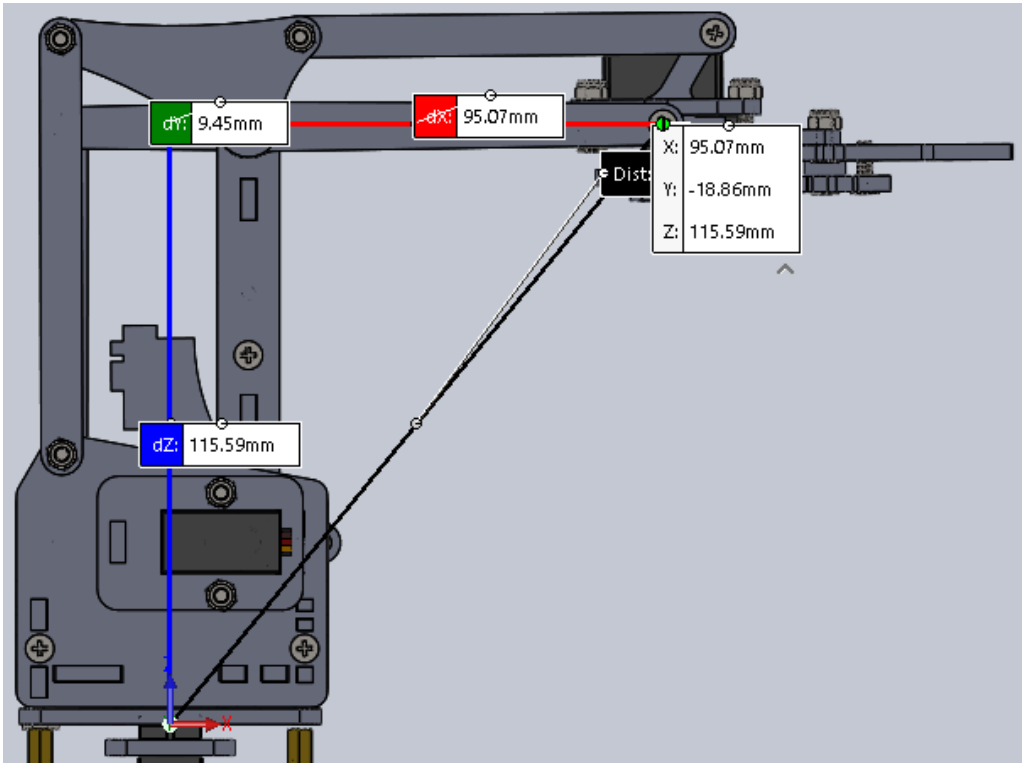

a

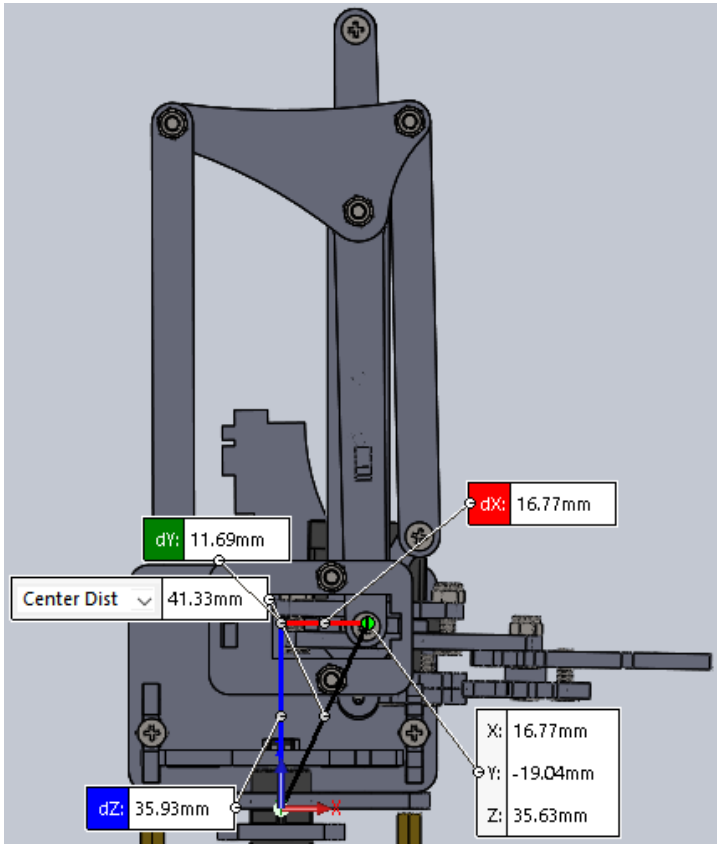

b

Fig. 5. Typical positions of the manipulator, which were simulated: a – $\varphi_2 = 0$, $\varphi_3 = 0$; b – $\varphi_2 = 0$, $\varphi_3 = 90°$

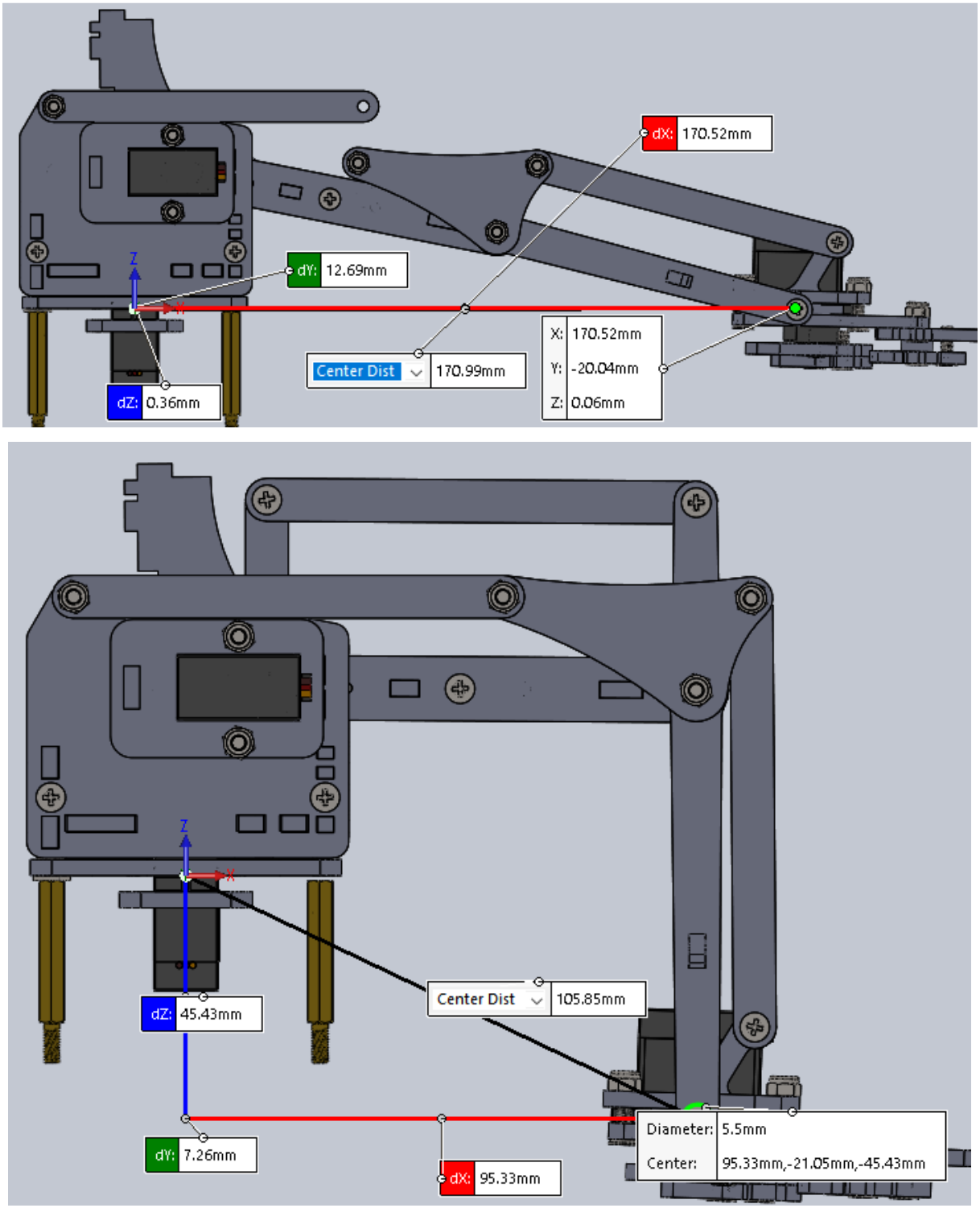

Fig. 5. (Continuation). Typical positions of the manipulator, which were simulated:
c – $\varphi_2 = 90°$, $\varphi_3 = 0$; d – $\varphi_2 = 90°$, $\varphi_3 = 90°$

Thus, analysing the graphical dependences (Fig. 3) obtained on the basis of analytical formulas (1) – (5) describing the kinematics of the manipulator, and comparing them with the simulation models of the gripper motion obtained with a help of SolidWorks software, we can note the complete matching of the results, which allows us to conclude on the adequacy of the derived analytical dependences (1) – (5).

In order to perform the overall investigation of kinematic parameters of the pantograph-type manipulator, let us carry out the simulation of its motion in MapleSim software.

Simulation of the Manipulator Motion in MapleSim Software

MapleSim is a Modelica-based, multi-domain modelling and simulation tool developed by Maplesoft. MapleSim generates model equations, runs simulations, and performs analyses using the symbolic and numeric mathematical engine of Maple. Models are created by dragging-and-dropping components from a library into a central workspace, resulting in a model that represents the physical system in a graphical form.

The MapleSim library includes many components that can be connected together to model a system. These components are from various areas of science and engineering, in particular from mechanical area. The use of Maple underneath MapleSim allows all of the system equations to be generated and simplified automatically. The user can explore their system in various ways, such as viewing the equations behind their model and performing parameter optimization.

The MapleSim model of the manipulator is presented in Fig. 4. It is constructed using 4 basic components that can be found in Multibody and 1-D Mechanical Libraries. Fixed Frame (point O) is a stationary frame with a fixed displacement and orientation relative to ground. Rigid Body Frame (e.g., OB_1, B_1B_2, B_2B_3 etc.) is a frame with a fixed displacement and orientation relative to a rigid body centre of mass (CoM) frame. Rigid Body (e.g., RB_1, RB_2, RB_3 etc.) is a centre of mass (CoM) frame with associated mass and inertia matrix. The Rotational Constant Speed (or Constant Speed) component (CS_1, CS_2) generates a fixed 1-D rotational constant speed at the flange.

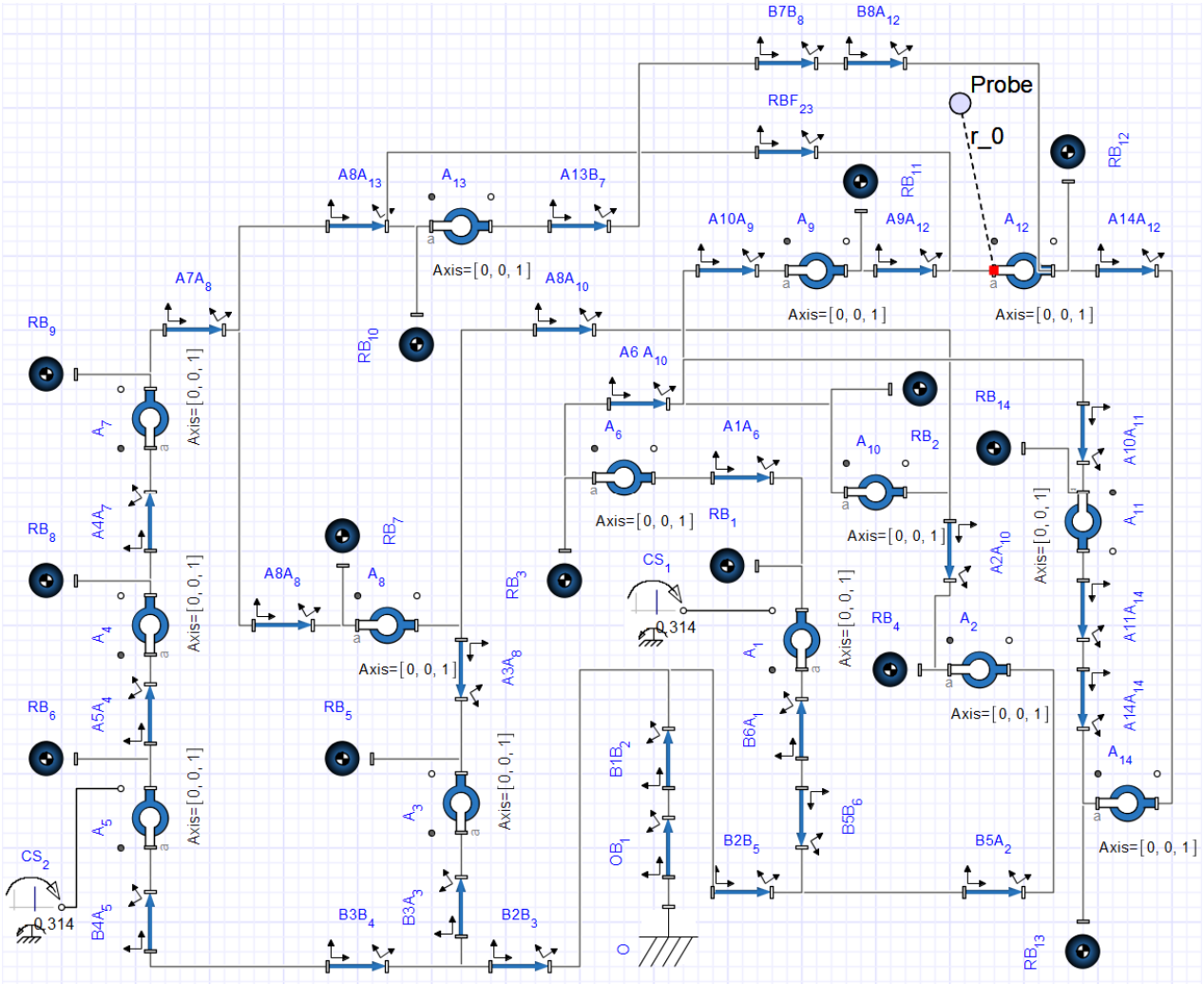

Fig. 6. MapleSim model of the manipulator

The four typical positions of the manipulator that correspond to the positions simulated in SolidWorks software were modelled in MapleSim 3-D Worspace and are presented in Figs. 7, a – d. In Fig. 7, a, there is shown the initial position of the manipulator, for which $\varphi_2 = 0$, $\varphi_3 = 0$, i.e. the driving rocker A_2A_{10} is in the vertical position, and the rocker A_4A_5 is in the horizontal position (see also Fig. 5, a). Fig. 7, b shows the position of the manipulator, for which $\varphi_2 = 90°$, $\varphi_3 = 0$, i.e. both driving rockers A_2A_{10} and A_4A_5 are in their horizontal positions (see also Fig. 5, c). In Fig. 7, c, there is shown the position of the manipulator, for which $\varphi_2 = 0$, $\varphi_3 = 90°$, i.e. both driving rockers A_2A_{10} and A_4A_5 are in their vertical positions (see also Fig. 5, b). In Fig. 7, d, there is shown the position of the manipulator, for which $\varphi_2 = 90°$, $\varphi_3 = 90°$, i.e. the driving rocker A_2A_{10} is in the horizontal position, and the rocker A_4A_5 is in the vertical position (see also Fig. 5, d).

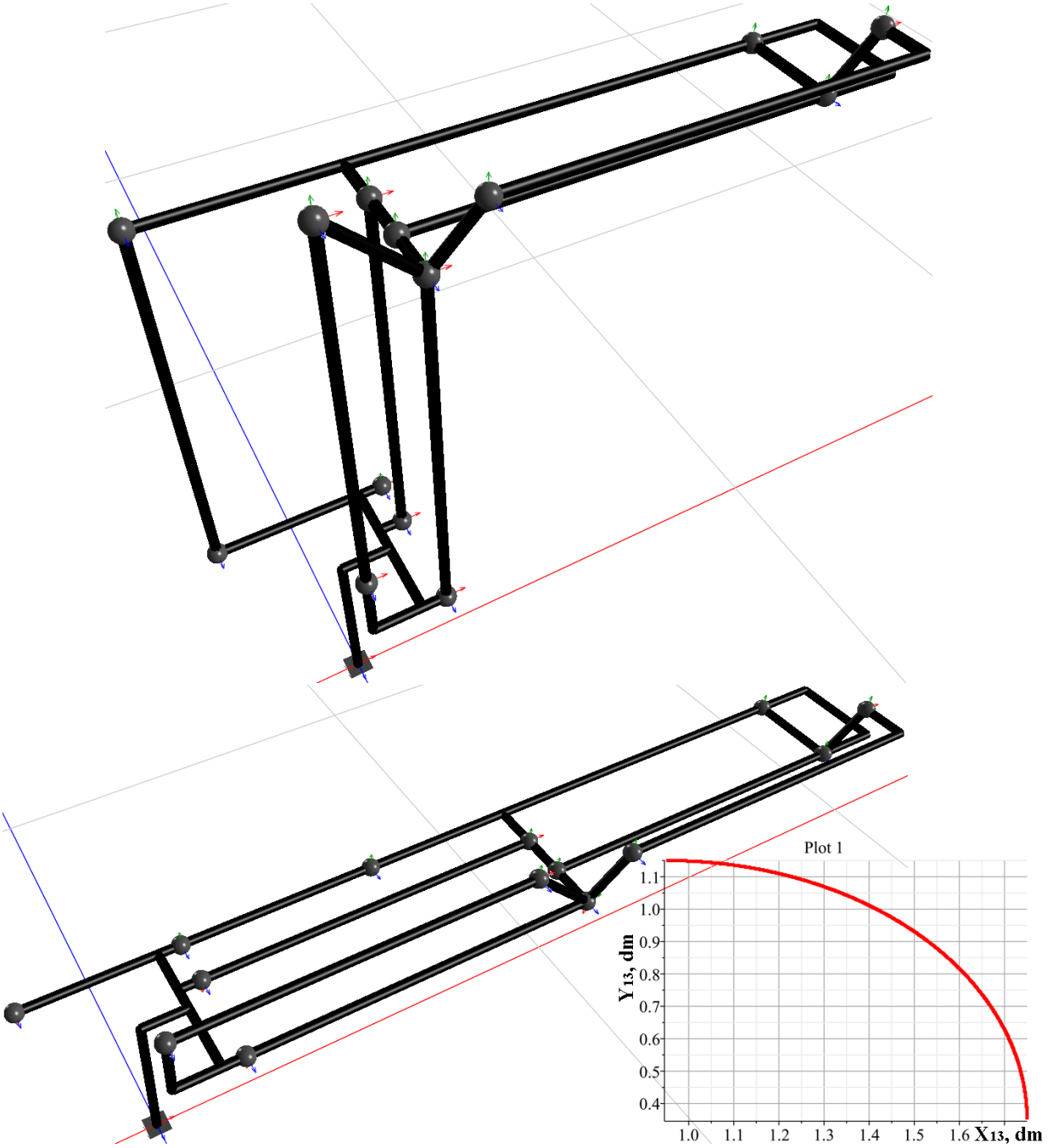

Fig. 7. Typical positions of the manipulator, which were simulated: a – $\varphi_2 = 0$, $\varphi_3 = 0$; b – $\varphi_2 = 90°$, $\varphi_3 = 0$

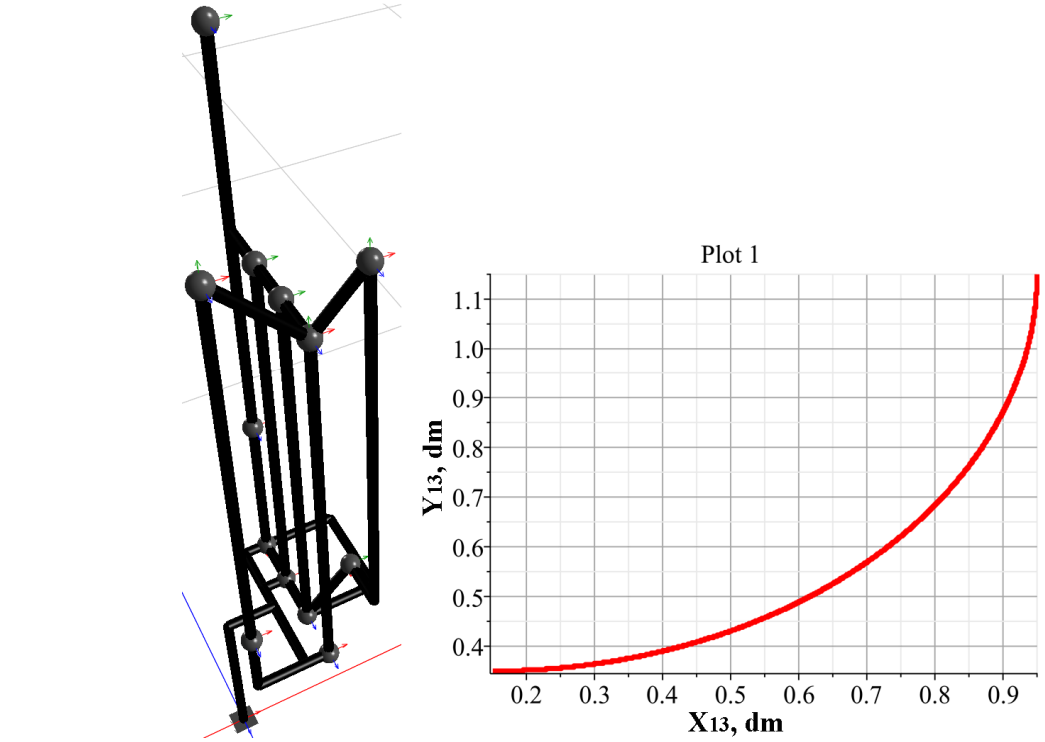

c

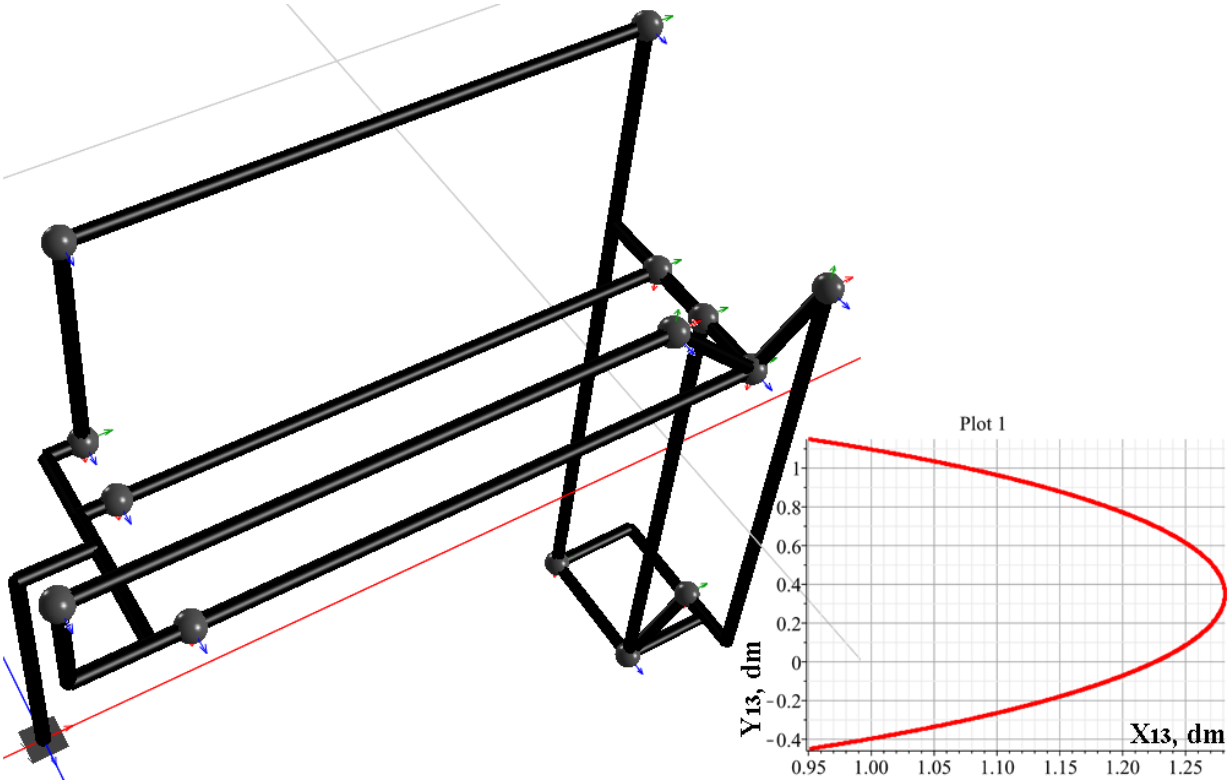

d

Fig. 7. (Continuation). Typical positions of the manipulator, which were simulated:
c – $\varphi_2 = 0$, $\varphi_3 = 90°$; d – $\varphi_2 = 90°$, $\varphi_3 = 90°$

Using MapleSim simulation software, there were modelled the typical movements of the manipulator from its initial position to the positions mentioned above. The obtained plots (Figs. 7, a – d) describing the trajectory (the path) of the gripper supporting point (A_{13}, Fig. 2) completely match the results of numerical modelling presented in Figs. 3, a – d, as well as the results of computer simulation of the manipulator motion performed in SolidWorks software and presented in Figs. 5, a – d.

Conclusions

The experimental sample of a mobile robotic system is designed in SolidWorks software and implemented in practice (see Fig. 1). Its structural and operational peculiarities are considered.

The structural and kinematic analysis of the manipulator is carried out, on the basis of which the number of its degrees of freedom is determined and the analytical dependences (1) – (5) describing the motion of the gripper are derived. According to the obtained results, the dependences of the coordinates of the gripper supporting point on the generalized coordinates φ_1, φ_2, φ_3 are derived (see Fig. 2). It is established that the generalized coordinate φ_1 describes the rotation of the manipulator around the vertical axis, while the coordinates φ_2, φ_3 describe the raising/lowering and pushing/pulling movements of the gripper.

Numerical modelling of the gripper motion is performed on the basis of the derived analytical dependences (1) – (5) using the MathLab software. There are presented the graphical dependences (see Figs. 3, a – d) presenting the changes of coordinates of the gripper supporting point while performing the characteristic movements which were selectively investigated in the course of numerical modeling: a – $\varphi_3 = 0$; b – $\varphi_2 = 0$; c – $\varphi_3 = 90°$; d – $\varphi_2 = 90°$.

The integrated kinematic analysis and simulation of the manipulator motion are performed on the basis of its solid-state model (see Fig. 4) designed in the SolidWorks software. The obtained results are presented in the form of characteristic positions of the manipulator with indication of the corresponding geometrical parameters (see Fig. 5). Based on the results of simulation, a conclusion is made about the complete matching of the results of analytical modelling and computer simulation, which allows us to prove the adequacy of the derived analytical dependences (1) – (5).

The simulation model of the manipulator that corresponds to its structure diagram (see Fig. 2) is constructed in MapleSim software (see Fig. 6). The corresponding movements of the links are modelled (see Figs. 7) and the obtained results are compared with the results of analytical calculations and simulation.

While carrying out further investigations, it is necessary to perform its dynamic analysis taking into account all the forces acting upon the elements of the robot, as well as the influence of drives. This will allow to carry out the optimization synthesis of the robots structure.

References

[1] I. J. Cox, G. T. Wilfong, *Autonomous Robot Vehicles*. New York: Spinger-Verlag, 1990.

[2] J. L. Jones, A. M. Flynn, B. A. Seiger, *Mobile Robots: Inspiration to Implementation*. Boka Raton, Fl: CRC Press, 2019.

[3] F. Fahimi, *Autonomous Robots: Modelling, Path Planning, and Control*. New York: Springer Science + Business Media, 2009.

[4] R. N. Jazar, *Theory of Applied Robotics: Kinematics, Dynamics, and Control*. New York: Springer Science + Business Media, 2010.

[5] P. Sandin, *Robot mechanisms and mechanical devices*. New York: McGraw-Hill, 2003.

[6] R. M. Murray, Z. Li, S. Sh.Sastry, *A Mathematical Introduction to Robotic Manipulation*. Boka Raton, Fl: CRC Press, 1994.

[7] C. D. Crane III, J. Duffy, *Kinematic Analysis of Robot Manipulators*. New York: Cambridge University Press, 2008.

[8] M. Ceccarelli, *Fundamentals of Mechanics of Robotic Manipulation*. Dordrecht, Netherlands: Kluwer Academic Publishers, 2004.

[9] J. Angeles, *Fundamentals of Robotic Mechanical Systems: Theory, Methods, and Algorithms*. Cham, Switzerland: Springer, 2014.

[10] J. J. Craig, *Introduction to Robotics Mechanics and Control*. Upper Saddle River, NJ: Pearson Education, 2005.

[11] H. Choset, et al., *Principles of Robot Motion: Theory, Algorithms, and Implementation*. Cambridge, MA: The MIT Press, 2005.

[12] A. J. Kurdila, P. Ben-Tzvi, *Dynamics and Control of Robotic Systems*. Hoboken, NJ: Wiley, 2019.

[13] K. Russell, Q. Shen, R. S. Sodhi, *Kinematics and Dynamics of Mechanical Systems Implementation in MATLAB® and SimMechanics®*. Boka Raton, Fl: CRC Press, 2019.

[14] D. B. Marghitu, *Mechanisms and Robots Analysis with MATLAB®*. London, UK: Springer-Verlag, 2009.